ABCM Symposium Series in Mechatronics - Vol. 4 - pp.854-863

On-line Trajectory Adaptation for Active Lower Limbs Orthoses based on Neural Networks

Marciel A. Gomes, gmarciel@sc.usp.br
University of São Paulo at São Carlos, Mechanical Engineering Department, Mechatronics Laboratory, Av. Trabalhador São-carlense, 400 - São Carlos, SP, Brazil

Guilherme L. M. Silveira, s_guilherme_lm@hotmail.com
University of São Paulo at São Carlos, Mechanical Engineering Department, Mechatronics Laboratory

Adriano A. G. Siqueira, siqueira@sc.usp.br
University of São Paulo at São Carlos, Mechanical Engineering Department, Mechatronics Laboratory

Abstract. *This work deals with on-line gait-pattern adaptation algorithms for an active lower limbs orthosis based on neural networks (NN). Stable trajectories are generated during the optimization process, considering a trajectory generator based on the Zero Moment Point criterion (ZMP) and the inverse dynamic model. Additionally, a set of neural networks are used to decrease the time-consuming computation of the model and ZMP optimization. The first neural network approximates the inverse dynamics and the ZMP, while the second one works in the optimization procedure, giving an adapted desired trajectory according to orthosis-patient interaction. This trajectory adaptation is added directly to the trajectory generator, also reproduced by a set of neural networks. With this strategy, it is possible to adapt the trajectory during the walking cycle in an on-line procedure, instead of changing the trajectory parameter after each step as it is performed in previous works. The dynamic model of the actual exoskeleton, with interaction forces included, is used to generate simulation results. The results show the proposed algorithm can be applied to an actual orthosis, since the computational cost is reduced with the use of neural networks.*

Keywords: *Exoskeleton, stable gait-pattern, adaptation algorithms, neural networks*

1. INTRODUCTION

The use of robotics as support for rehabilitation procedures is increasing due mainly to the importance of exercises for functional rehabilitation (Ferris, Sawicki and Domingo, 2005). The robotic orthosis Lokomat is being used for rehabilitation of patients with stroke or spinal cord injury individuals (Jezernik, Colombo, Keller, Frueh and Morari, 2003). The device is installed in a treadmill and the patient walks using a weight compensator and performing a fixed gait-pattern, imposed through a joint position control of the robotic orthosis. Gait-pattern adaptation algorithms, based on the human-machine interaction, are proposed in (Jezernik, Colombo and Morari, 2004, Riener, Lünenburger, Jezernik, Anderschitz, Colombo and Dietz., 2005) to ensure the patient is not only having its leg moved passively for the locomotion device.

However, the proposed algorithms in (Riener et al., 2005) can not be applied directly for active lower limbs orthoses since they were developed for a fixed base robotic system, the Lokomat orthosis. They do not consider the stability of the gait-pattern. For exoskeleton, which can be considered as a biped robot, the generation of a stable walking pattern is an essential issue. In (Huang, Yokoi, Kajita, Kaneko, Arai, Koyachi and Tanie, 2001), it is presented a trajectory generator for biped robots taking into account the ZMP criterion (Vukobratovic and Juricic, 1969). Specific points of the ankle and hip trajectories are defined according to the desired step length and duration, and the minimization of a functional related to the ZMP. The cubic splines interpolation method is used to generate the smooth and second-order differentiable curves, and the joint trajectories are obtained from inverse kinematics. In (Mousavi, Nataraj, Bagheri and Entezari, 2008), the trajectory generator proposed in (Huang et al., 2001) is extended for different ground inclinations and stairs.

In this paper it is proposed the application of the inverse dynamic-based gait-pattern adaptation algorithm proposed in (Riener et al., 2005) considering the stable trajectory generator described in (Huang et al., 2001). In this way, stable trajectories are generated during the optimization process where the step duration, considered here as the adaptation parameter, is updated according to the orthosis-patient interaction. Furthermore, a set of neural networks is used to decrease the time-consuming computation of the model and ZMP optimization trough an on-line adaptation strategy. The first NN works as function approximator of the model-dependent term, while the second one works as part of the optimization procedure and gives the adapted parameter. A third NN replaces the trajectory generator in such a way that the ZMP optimization (also a time-consuming computation) is performed on-line according to the value of the adapted parameter. This strategy is different from the one presented in (Gomes and Siqueira, 2009), since in that case the ZMP optimization is preformed after the step is completed.

To ensure the orthosis-patient system follows the desired trajectory even in the presence of external disturbances and parametric uncertainties, a robust controller based on $\mathscr{H}_\infty$ performance is implemented. In (Siqueira and Terra, 2004), the authors present experimental results obtained from the implementation in robot manipulators of a nonlinear $\mathscr{H}_\infty$ control

ABCM Symposium Series in Mechatronics - Vol. 4 - pp.854-863

via quasi-linear parameter varying (quasi-LPV) representation. The quasi-LPV representation of a nonlinear system is a state-space equation where the system matrices are functions of state-dependent parameters (Wu, Yang, Packard and Becker, 1996). In (Siqueira and Terra, 2006), a similar controller is proposed for disturbance attenuation considering a semi-passive dynamic walking of biped robots.

The paper is organized as follows: Section 2. presents the trajectory generator for biped robots; Section 3. presents the dynamic model of the orthosis-patient system and the robust controller design; Section 4. introduces the gait-pattern adaptation algorithm based on inverse dynamics applied to exoskeletons; Section 5. presents the neural networks' structures and the complete description of the optimization process; Section 6. presents the simulated results of the gait-pattern adaptation algorithm applied to an exoskeleton model; and Section 7. shows the conclusions.

2. TRAJECTORY GENERATION WITH ZMP CRITERION

In this section, the trajectory generator for biped robots proposed in (Huang et al., 2001) is presented, with some considerations about the ZMP trajectory optimization. The exoskeleton is considered as a biped robot with trunk, knees and feet, as shown in Figure 1. According to (Huang et al., 2001), the walking cycle can be divided in two phases, double support and single support. The double support phase starts when the heel of the forward foot touches the ground and finishes when the toe of the backward foot leaves the ground. The second phase is characterized by the fact only one foot is in contact with the ground. In this work, the double support represents 20% of the entire walking cycle.

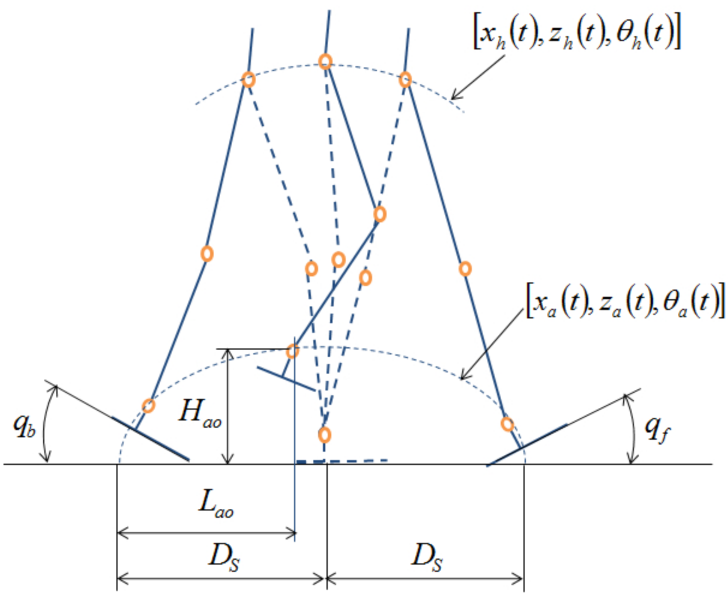

Figure 1. Biped robot model.

Consider the inertia coordinate system of Figure 1. The foot and hip trajectories can be respectively parametrized as $X_a = [x_a(t), z_a(t), \theta_a(t)]^T$, where $(x_a(t), z_a(t))$ is the ankle position and $\theta_a(t)$ is the angle between the foot and the horizontal plane, and $X_h = [x_h(t), z_h(t), \theta_h(t)]^T$, where $(x_h(t), z_h(t))$ is the hip position and $\theta_h(t)$ is the angle between the trunk and the horizontal plane.

2.1 Foot Trajectory

The step k occurs between the kT_c and $(k+1)T_c$ time instants, where T_c is the step time interval. Step k is defined starting when the heel of any foot leaves the ground and finishing when the same heel touches the ground again, Figure 2. q_b and q_f are the angles of the foot with relation to the horizontal at the initial and final time instants of the swing phase (single support), respectively.

Assuming that the left foot is completely in contact with the ground during the times $kT_c + T_d$ and $(k+1)T_c$, the following conditions can be stated:

$$\theta_a = \begin{cases} q_{gs}(k), & t = kT_c \\ q_b, & t = kT_c + T_d \\ -q_f, & t = (k+1)T_c \\ -q_{ge}(k), & t = (k+1)T_c + T_d \end{cases} \tag{1}$$

where T_d is the time interval of the double support phase, $q_{gs}(k)$ and $q_{ge}(k)$ are the ground slope for the initial and final step instants, respectively.

ABCM Symposium Series in Mechatronics - Vol. 4 - pp.854-863

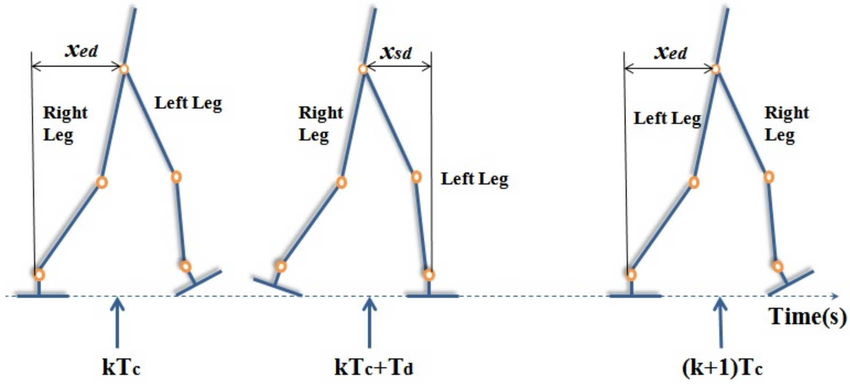

Figure 2. Walking cycle, double and single support phases.

The following specifications can also be defined for the foot position:

$$x_a = \begin{cases} kD_s, & t = kT_c \\ kD_s + l_{an}sin(q_b) + l_{af}(1 - cos(q_b)), & t = kT_c + T_d \\ kD_s + L_{ao}, & t = kT_c + T_m \\ (k+2)D_s - l_{an}sin(q_f) - l_{ab}(1 - cos(q_f)), & t = (k+1)T_c \\ (k+2)D_s, & t = (k+1)T_c + T_d \end{cases} \tag{2}$$

and

$$z_a = \begin{cases} h_{gs}(k) + l_{an}, & t = kT_c \\ h_{gs} + l_{af}sin(q_b) + l_{an}cos(q_b), & t = kT_c + T_d \\ H_{ao}, & t = kT_c + T_m \\ h_{ge} + l_{ab}sin(q_f) + l_{an}cos(q_f), & t = (k+1)T_c \\ h_{ge}(k) + l_{an}, & t = (k+1)T_c + T_d \end{cases} \tag{3}$$

where $(kD_s + L_{ao}, H_{ao})$ is the higher foot position during the step (this position occurs at $kT_c + T_m$), D_s is the half step length, l_{an} is the foot height and l_{af} is the distance between the heel and the ankle joint. The heights of the ground when the foot is touching it are defined as $h_{gs}(k)$ and $h_{ge}(k)$, for the initial and final step instants, respectively. Some constraints on right foot velocities are also imposed, see (Huang et al., 2001) for details.

A smooth trajectory can be generated through the interpolation method based on cubic splines, which generates a second order differentiable trajectory for all time interval.

2.2 Hip Trajectory

It is considered that the angle between the trunk and the horizontal axis $\theta_h(t)$ presents no variation along the walking cycle. Also, as the position of the ZMP is not affected by the hip motion in the z direction, it is assumed a little variation between the highest position H_{hmax} and the lowest position H_{hmin}, where the former occurs at the middle of the single support phase and the second at the middle of the double support phase. That is, z_h can be defined as:

$$z_h = \begin{cases} H_{hmin}, & t = kT_c + 0,5T_d \\ H_{hmax}, & t = kT_c + 0,5(T_c - T_d) \\ H_{hmin}, & t = (k+1)T_c + 0,5T_d. \end{cases} \tag{4}$$

Considering the sagittal plane, the hip motion along the x direction is the main contribution for the ZMP be inside the support polygon. In (Huang et al., 2001) it is proposed generate a set of stable trajectories $x_h(t)$ and select the trajectory with large stability margin according to the ZMP criterion.

The following conditions are defined for the hip trajectory along the x direction:

$$x_h = \begin{cases} kD_s + x_{ed}, & t = kT_c \\ (k+1)D_s - x_{sd}, & t = kT_c + T_d \\ (k+1)D_s + x_{ed}, & t = (k+1)T_c \end{cases} \tag{5}$$

where x_{sd} and x_{ed} are the distances along the x direction from the hip to the ankle of the support foot at the initial and final time instants of the swing phase, respectively, Figure 2. In this paper, these values are constrained to $x_{sd} \in (0; 0.5D_s)$ and $x_{ed} \in (0; 0.5D_s)$.

ABCM Symposium Series in Mechatronics - Vol. 4 - pp.854-863

Considering the interpolation method based on cubic splines, it is possible to generate different trajectories and to select the best one according to the ZMP criteria. To guarantee that the ZMP remains most of the time next to the center to the support polygon, the following functional is defined:

$$J_{zmp}(x_{ed},x_{sd}) = \frac{\sum_{n=1}^{p} d_{zmp}^2}{p}, \tag{6}$$

where d_{zmp} is the distance between the ZMP and the center of the stability region defined by the convex polygon of the contact points and p is the number of points throughout the trajectory in which d_{zmp} is computed.

2.3 Optimization Issues

The steepest descent algorithm was selected as the optimization method to minimize the functional (6). It presents a easy implementation and high convergence rate after all parameters be adjusted. The computation of J_{zmp} is highly time consuming if a representative number of trajectory points p must be considered. The algorithm is defined as:

$$\overline{X}_{n+1} = \overline{X}_n - \eta \nabla J(x_{ed},x_{sd}) \tag{7}$$

where $\overline{X}_n$ is the vector containing the values of x_{ed} and x_{sd} for optimization step n, η is the optimization rate and $\nabla J_{zmp}(x_{ed},x_{sd})$ is the functional gradient with relation to x_{ed} and x_{sd}.

From the analysis of the variation of J_{zmp} given a variation of D_s, it is proposed a relation between the step length, D_s, and the maximum height, H_{hmax}. For a given D_s, H_{hmax} can be computed as the height of the isosceles triangle defined by base D_s and sides $L_{th}+L_{sh}$ plus the ankle height. This value is parametrized by parameters defined as function of $(Ds-0.5)$ an $(Tc-0.9)$, the differences from the initial values of D_s and T_c, as shown in the following equations:

$$H_{hmax} = \left(\sqrt{(L_{sh}+L_{th})^2 - \left(\frac{D_s}{2}\right)^2} + l_{an}\right).\alpha_1.\alpha_2, \tag{8}$$

$$\begin{cases} \alpha_1 = \left(\frac{D_s-0.5}{0.5}\right)^2 - 1, & D_s - 0.5 > 0, \\ \alpha_1 = 1, & D_s - 0.5 < 0, \end{cases} \tag{9}$$

$$\alpha_2 = \left(\frac{|T_c - 0.9|}{0.9}\right)^{3.2} - 1. \tag{10}$$

where L_{sh} and L_{th} are the lengths of the shin and thigh, respectively.

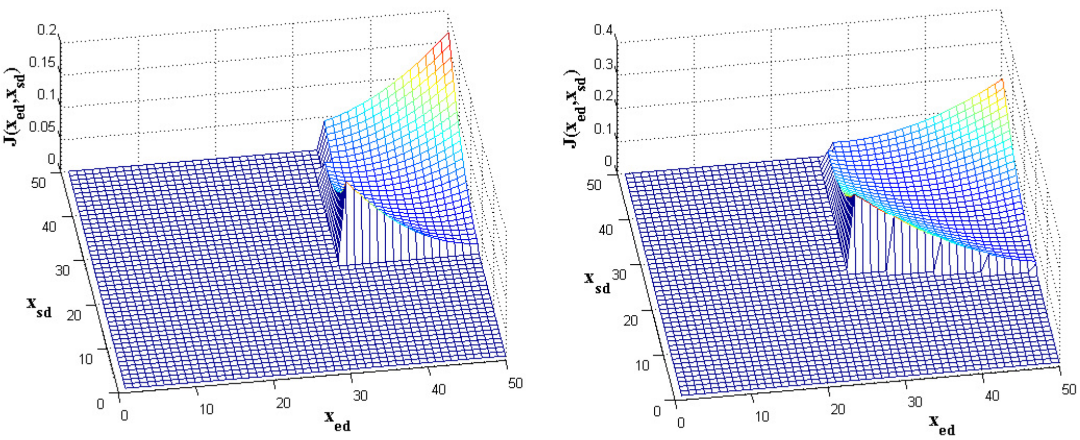

Figure 3. Surfaces for J considering the empiric relation for H_{hmax}.

Figure 3 shows the surfaces for J_{zmp} computed for different values of D_s and considering the empirical relation for H_{hmax}. Note that the functional domain remains suitable for the optimization, even with the variation of D_s.

ABCM Symposium Series in Mechatronics - Vol. 4 - pp.854-863

3. ORTHOSIS-PATIENT DYNAMICS AND ROBUST CONTROL DESIGN

To implement the robust controller and the gait-pattern adaptation algorithm, the orthosis is modeled according to the basic robotic equation,

$$M_{ort}(q)\ddot{q}+C_{ort}(q,\dot{q})+G_{ort}(q)=\tau_a+\tau_{pat}+\tau_d, \tag{11}$$

where $q \in \Re^n$ is the generalized coordinates vector, $M \in \Re^{nxn}$ is the symmetrical, positive definite inertia matrix, $C \in \Re^n$ is the centrifugal and Coriolis torques vector, and $G \in \Re^n$ is the gravitational torques vector. The terms $\tau \in \Re^n$ are the torques acting in orthosis: τ_a is the torque supplied by the actuators, τ_{pat} is the torque generated for the orthosis-patient interaction, and τ_d is the torque generated by any external disturbances acting in the patient-orthosis system.

The torque of interaction between the orthosis and the patient, τ_{pat}, can be divided in active and passive components. The passive patient torque, $\tau_{pat,pas}$, is the torque necessary to move the patient if he/she is moving in a passive way. In case that the patient influences in the orthosis movement, he/she will produce the active patient torque, $\tau_{pat,act}$. Therefore, Eq. (11) can be rewrite, considering now, the orthosis-patient dynamics,

$$\begin{aligned} M_{ort+pat}(q)\,\ddot{q}+C_{ort+pat}(q,\dot{q})+G_{ort+pat}(q) \\ =\tau_a+\tau_{pat,act}+\tau_d, \end{aligned} \tag{12}$$

where $M_{ort+pat}(q)$, $C_{ort+pat}(q,\dot{q})$, and $G_{ort+pat}(q)$ corresponds to the combination of the orthosis and patient dynamics.

Also, the state tracking error is defined as:

$$\tilde{x}=\begin{bmatrix}\dot{q}-\dot{q}^d\\ q-q^d\end{bmatrix}=\begin{bmatrix}\dot{\tilde{q}}\\ \tilde{q}\end{bmatrix} \tag{13}$$

where q^d and $\dot{q}^d \in \Re^n$ are the desired reference trajectory and the corresponding velocity, respectively. The variables q^d, $\dot{q}^d$ and $\ddot{q}^d$, the desired acceleration, are assumed to be within the physical and kinematics limits of the robot.

The dynamic equation for the tracking error is given from (12) and (13) as

$$\dot{\tilde{x}}=A(q,\dot{q})\tilde{x}+Bu+Bw \tag{14}$$

with

$$\begin{aligned} A(q,\dot{q})&=\begin{bmatrix}-M^{-1}_{ort+pat}(q)C_{ort+pat}(q,\dot{q}) & 0\\ I_n & 0\end{bmatrix},\\ B&=\begin{bmatrix}I_n\\ 0\end{bmatrix},\\ w&=M^{-1}_{ort+pat}(q)\delta(q,\dot{q},\ddot{q}),\\ u&=M^{-1}_{ort+pat}(q)(\tau-M_{ort+pat}(q)\ddot{q}^d-C_{ort+pat}(q,\dot{q})\dot{q}^d-G_{ort+pat}(q)), \end{aligned}$$

where $\delta(q,\dot{q},\ddot{q})$ are the composed disturbances defined as the sum of the external disturbances, τ_d, and the parametric uncertainties on the dynamic matrices $M_{ort+pat}(q)$, $C_{ort+pat}(q,\dot{q})$ and $G_{ort+pat}(q)$. The applied torque is given by:

$$\tau=M_{ort+pat}(q)(\ddot{q}^d+u)+C_{ort+pat}(q,\dot{q})\dot{q}^d+G_{ort+pat}(q).$$

Actually, the robust controller is working to attenuate only the effects of the external disturbances and the parametric uncertainties on the trajectory tracking errors. The active patient torque, $\tau_{pat,act}$, is not included into the composed disturbances, $\delta(q,\dot{q},\ddot{q})$, since it will be attenuated by the gait-pattern adaptation algorithm.

3.1 State-feedback $\mathscr{H}_\infty$ Control Design

In this section it is presented the formulation and solution for the state-feedback $\mathscr{H}_\infty$ control problem for quasi-LPV systems, where the varying parameters are function of the system states.

The tracking error dynamics shown in Eq.(14) is actually a quasi-LPV system, since, although the matrix $M_{ort+pat}(q)$ explicitly depends on the joint positions, we can consider it as function of the position error (Siqueira and Terra, 2004):

$$M_{ort+pat}(q)=M_{ort+pat}(\tilde{q}+q^d)=M_{ort+pat}(\tilde{x},t).$$

The same can be observed for $C_0(q,\dot{q})$.

ABCM Symposium Series in Mechatronics - Vol. 4 - pp.854-863

Then, consider the state-feedback control problem

$$\begin{aligned} \dot{x} &= A(\rho(x))x + B_1(\rho(x))w + B_2(\rho(x))u, \\ z_1 &= C_1(\rho(x))x, \\ z_2 &= C_2(\rho(x))x + u \end{aligned} \tag{15}$$

where $x \in \Re^n$ is the state, $u \in \Re^{q_2}$ is the control input, $w \in \Re^p$ is the disturbance input, $z_1 \in \Re^{q_1}$ and $z_2 \in \Re^{q_2}$ are system outputs, $A(\cdot)$, $B_1(\cdot)$, $B_2(\cdot)$, $C_1(\cdot)$ and $C_2(\cdot)$ are continuous matrices of proper dimensions and $\rho(x) \in F_P^\nu$, defined by

$$F_P^\nu = \left\{\rho \in \mathscr{C}^1(\Re^+, \Re^m) : \rho(x) \in P,\, |\dot{\rho}_i| \le \nu_i, i = 1, \ldots, m\right\},$$

where $P \subset \Re^m$ is a compact set, and $\nu = [\nu_1 \cdots \nu_m]^T$ with $\nu_i \ge 0$. The system (15) presents $\mathscr{L}_2$ *gain* $\le \gamma$ in the interval $[0, T]$ if

$$\int_0^T \|z(t)\|_2^2 dt \le \gamma^2 \int_0^T \|w(t)\|_2^2 dt, \tag{16}$$

for all $T \ge 0$, all $w \in \mathscr{L}_2(0,T)$ with the system starting from $x(0) = 0$ and $z(t) = [z_1(t)^T \;\; z_2(t)^T]^T$. The objective is to find a continuous function $F(\rho(x))$, such that the system in closed-loop presents $\mathscr{L}_2$ *gain* $\le \gamma$ with state-feedback law $u = F(\rho(x))x$. This problem was solved in (Wu et al., 1996) and the solution is given in the following.

If there exists a continuous differentiable function $X(\rho(x)) > 0$ for all $\rho(x) \in P$ that satisfies

$$\begin{bmatrix} G(\rho) & X(\rho)C_1^T(\rho) & B_1(\rho) \\ C_1(\rho)X(\rho) & -I & 0 \\ B_1^T(\rho) & 0 & -\gamma^2 I \end{bmatrix} < 0, \tag{17}$$

where

$$G(\rho) = -\sum_{i=1}^m \pm\left(\nu_i \frac{\partial X}{\partial \rho_i}\right) + \widehat{A}(\rho)X(\rho) + X(\rho)\widehat{A}^T(\rho) - B_2(\rho)B_2^T(\rho)$$

and $\widehat{A}(\rho) = A(\rho) - B_2(\rho)C_2(\rho)$, then, with state-feedback law

$$u = -(B_2^T(\rho)X^{-1}(\rho) + C_2(\rho))x, \tag{18}$$

the closed-loop system has $\mathscr{L}_2$ *gain* $\le \gamma$ for all parameter trajectories $\rho(x) \in F_P^\nu$.

Note that Eq.(17) actually represents 2^m inequalities and $\sum \pm(\cdot)$ indicates that every combination $+(\cdot)$ and $-(\cdot)$ should be satisfied. A practical scheme ((Wu et al., 1996, Siqueira and Terra, 2004)) can be used to solve the infinite dimensional convex optimization problem represented by Eq.(17). First, choose a set of $\mathscr{C}^1$ functions, $\{f_i(\rho(x))\}_{i=1}^M$, as base for $X(\rho)$, i.e.,

$$X(\rho(x)) = \sum_{i=1}^M f_i(\rho(x))X_i,$$

where $X_i \in S^{n \times n}$ is the matrix coefficient for $f_i(\rho(x))$.

Second, the parameters set P is divided in L points, $\{\rho_k\}_{k=1}^L$, in each dimension. Since (17) consists in 2^m entries, a total of $(2^m + 1)L^m$ matrix inequalities in term of matrices $\{X_i\}$ should be solved.

4. GAIT-PATTERN ADAPTATION ALGORITHM

In this section, an adaptation algorithm is used to generated the trajectory parameter T_c, according to the interaction between the orthosis and the patient.

Considering Eq. (12), the proposed algorithm, based on the inverse dynamics of the orthosis-patient system, works by minimizing the following functional,

$$J(\delta q_r, F) = \sum \left\| \tau_{pat,act}(F)_{(k)} - \delta\tau(\delta q_r)_{(k)} \right\|_2^2, \tag{19}$$

where F is the interaction forces between patient and orthosis and δq_r is the reference trajectory change due to T_c variation (Riener et al., 2005). The torque variation produced by a change in the reference trajectory, $\delta\tau(\delta q_r)$, is computed from

ABCM Symposium Series in Mechatronics - Vol. 4 - pp.854-863

the orthosis-patient dynamics as

$$\begin{aligned}\delta\tau(\delta q_r) =& M_{ort+pat}(q_r+\delta q_r)\left(\ddot{q}_r+\ddot{\delta}q_r\right)\\ &+C_{ort+pat}\left(q_r+\delta q_r,\dot{q}_r+\dot{\delta}q_r\right)\\ &+G_{ort+pat}(q_r+\delta q_r)-M_{pat,ort}(q_r)\ddot{q}_r\\ &-C_{pat,ort}(q_r,\dot{q}_r)-G_{pat,ort}(q_r),\end{aligned}$$

where q_r, $\dot{q}_r$ and $\ddot{q}_r$ are the reference trajectory and its first and second derivatives, respectively.

5. NEURAL NETWORK SYSTEM

The main contribution of this work is a neural network system for the optimization system that employs three Multilayer Perceptron NNs, Figure 4. The first NN is trained off-line using the orthosis-patient dynamics and the reference trajectory change, δq_r, to give the torque variation, $\delta\tau(\delta q_r)$. The use of the NN to approximate the torque variation is justified because, in this case, the ZMP optimization is not analytically performed. This procedure is time-consuming.

The three input neurons for this first NN are related to the current value of T_c ($T_{c_{actual}}$), the adapted value of T_c ($T_{c_{adapt}}$) and time, t. Also, 10 hidden neurons and 7 output neurons, related to the torque variation to the each joint, completes the NN structure. The following parameters were considered during the training stage (3000 epochs): $t\in[0;0.90]$ s; $T_{c_{actual}}, T_{c_{adapt}}\in[0.80;0.90]$ s; learning rate, $\alpha=0.30$ and momentum, $\gamma=0.89$. It is necessary to include the current value of the step time, $T_{c_{actual}}$, since, in every optimization step, $\delta\tau(\delta q_r)$ is computed as a variation from the current trajectory.

The second NN is trained on-line, during the swing phase. The objective of this NN is to find $T_{c_{adapt}}$ that minimizes the functional J, Eq.(19). Hence, the input to the backpropagation phase is the gradient of J with relation to $T_{c_{adapt}}$. This value is computed using the first NN. The input value for the second NN is $T_{c_{actual}}$, the current value of the step time, and the output is $T_{c_{adapt}}$, the adapted value. This NN is composed by 10 hidden neurons and the convergence occurs after 10 epochs. Both NNs use logistic activation function for all neurons. The inputs and outputs were normalized using max and min values for each variable.

Finally, the third NN reproduces the trajectory generator, decreasing the time consumed in the ZMP optimization. Actually, there is a NN for each joint variable: position , velocity and acceleration. The inputs of the NNs are the current time t and the adapted value of the step time, $T_{c_{adapt}}$. The structure of these NNs are defined by two input neurons, two hidden layers with 12 neurons for each one and 7 output neurons, related to the 7 joints being controlled.

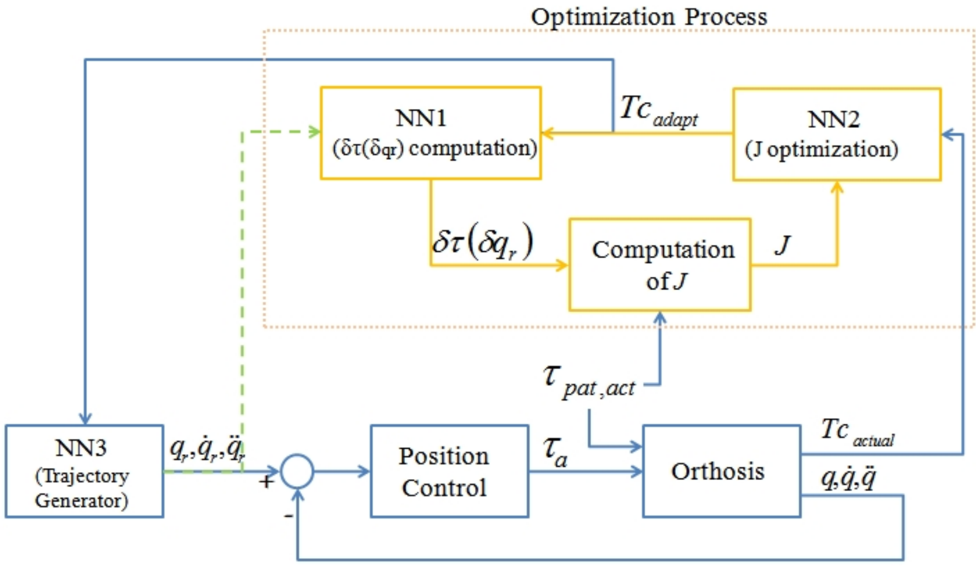

Figure 4. Structure of Neural Network-based system.

The overall adaptation process performs as follow: after generates a reference trajectory by initial parameters, the first NN (NN1 in the Figure 4) computes the torque variation, $\delta\tau(\delta q_r)$, which in together with the interaction torques provided by the patient results in the functional, J; this functional is minimized in the second NN (NN2) through its training process, ending up the adapted step time, $T_{c_{adapt}}$; this parameter, together with the current time instant, are the inputs of the third NN (NN3) which generates the desired trajectory (changing the reference trajectory).

The optimization is performed during the walking step with a specific numbers of trajectory points. Actually, it is

ABCM Symposium Series in Mechatronics - Vol. 4 - pp.854-863

considered the optimization occurs every ten sampling periods and starts when the swing leg becomes parallel to the support leg, taking into account the values of $\delta\tau(\delta q_r)$ and $\tau_{pat,act}$ at the trajectory points of the previous interval.

6. SIMULATION RESULTS

The orthosis used for the exoskeleton for lower limbs corresponds to one Reciprocating Gait Orthosis LSU (Lousiana State University). Figure 5 shows the orthosis and the exoskeleton design. It is considered that all joint in the sagittal plane will be driven by an Series Elastic Actuator (SEA). SEA can performed force and impedance controls, which can be used to generate a variable impedance controller (Walsh, Paluska, Pasch, Grand, Valiente and Herr, 2006).

Figure 5. Orthosis and exoskeleton design (Solid Edge).

The dynamic parameters of the orthosis, shown in Tab. 1, was obtained by the Solid Edge model. It is also presented the parameters of the patient considered in the simulation, obtained from (Winter, 1990), considering a 85 kg, 1.74 m individual. An analytical model of the orthosis, considering the patient interaction and ground reaction forces, is developed using the Symbolic Toolbox of the Matlab. Figure 6 shows the motion animation of the orthosis-patient system for a simulation of two steps. In the initial step it is considered $D_s = 0.45$ m and $T_c = 0.9$ s. For the second step $D_s = 0.58$ m and $T_c = 0.8$ s. Only the orthosis representation is shown since the patient dynamic is incorporated in the orthosis dynamics.

Table 1. Orthosis and Patient Dynamic Parameters.

Orthosis		**Patient**	
$M_{total,ort}$	4.8	$M_{total,pat}$	85
$L_{total,ort}$	1.0	$L_{total,pat}$	1.74
Limb Mass (kg)			
$M_{tigh,ort}$ 0.95		$M_{tigh,pat}$	8.5
$M_{leg+foot,ort}$	0.72	$M_{leg+foot,pat}$	5.2
$M_{torso,ort}$	1.49	$M_{torso,pat}$	57.6
Limb Length (m) - z direction			
$L_{tigh,ort}$	0.39	$L_{tigh,pat}$	0.39
$L_{leg+foot,ort}$	0.49	$L_{leg+foot,pat}$	0.49
$L_{torso,ort}$	0.12	$L_{torso,pat}$	0.87

In this section, the neural network-based gait-pattern adaptation algorithm presented in Sections 4. and 5. is implemented in the model of the orthosis of Fig. 5. The initial desired trajectory, considered here as the nominal one, is defined by $D_s = 0.5$ m and $T_c = 0.9$ s.

Because only simulation is performed in this work, the interaction torque between orthosis and patient (active patient torque) must be artificially estimated from a pre-specified trajectory. In this work, this value is computed through the comparison between the desired trajectory for the patient, q^d_{pat} and the actual desired trajectory, q^d. It is assumed that the interaction torque results of a spring type virtual coupling between the patient desired position and the real position,

$$\tau_{pat,act} = K\left(q^d_{pat} - q^d\right). \tag{20}$$

As the gait-pattern adaptation is performed on-line, the adapted trajectory reaches the desired one during the first step. To show the adaptation effectiveness of the NN-based algorithm, two simulations were performed. In the first one, the desired trajectory of the patient is defined by $T_c = 0.82$ s for all time steps. Figure 7(a) presents the nominal, patient

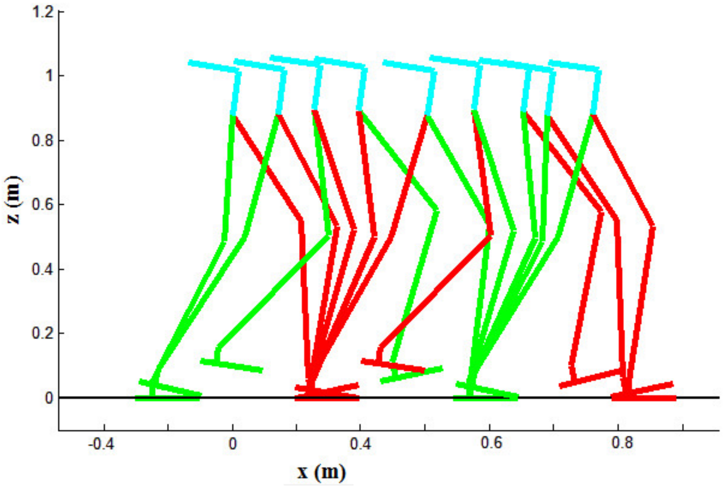

Figure 6. Motion animation of the orthosis-patient system.

desired, actual and adapted trajectories of the right tibia, referring three steps, initiating with the right leg in stance. Note that after the swing leg passes trough the vertical line (approximately, $t = 0.5$ s), the adapted trajectory comes close to the patient desired trajectory and follows it. In the second simulation, the desired T_c changes to 0.82 s, 0.86 s and 0.81 s, during the steps 1, 2 and 3, respectively. The adaptation occurs from the middle of each step. Figure 7(b) presents the nominal, patient desired, actual and adapted trajectories of the right tibia for the latter simulation. Note that, in all cases, the adaptation is performed efficaciously, with the trajectory changing according to the news parameters.

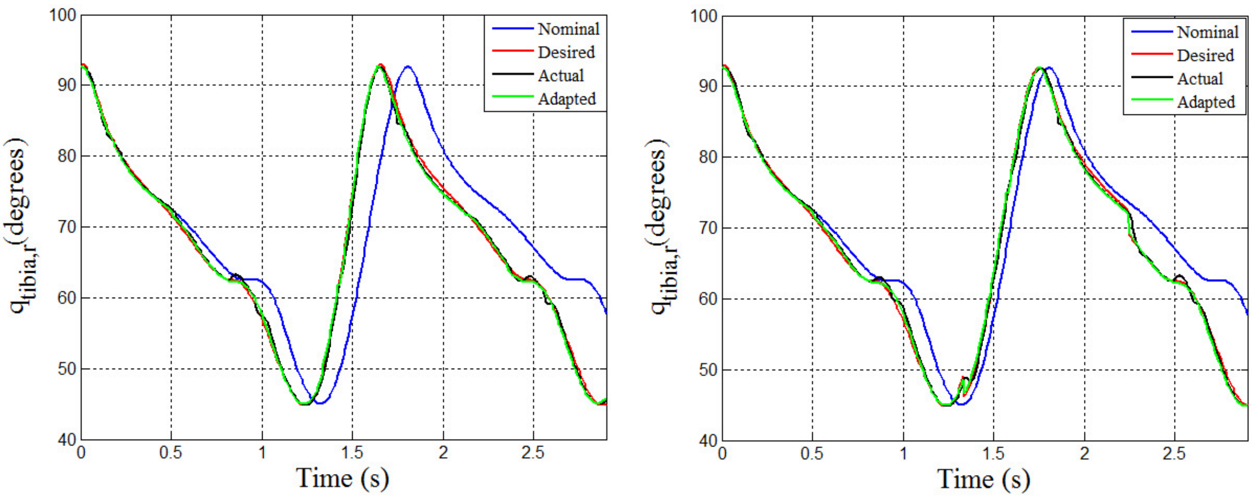

(a) Fixed desired T_c. (b) Variable desired T_c.

Figure 7. Nominal, patient desired, actual and adapted trajectories of the rigth tibia, absolute angle.

It was also observed that the proposed NN-based algorithm presents a decrease of approximately 70% in the processing time, compared with the model-based algorithms. The results show that the proposed NN-based algorithm is suitable for application in an actual active orthosis.

External disturbances acting in the patient-orthosis joints can be simulated as additional torques applied to the actuators. In this paper, it is considered in the simulation external disturbances composed of normal and sine functions, see (Siqueira and Terra, 2006) for details. From Figures 7(a) and 7(b) it can be verified that the robust controller rejected the external disturbances applied at the initial part of each step.

7. CONCLUSIONS

This paper presents a on-line neural network-based gait-pattern adaptation algorithm which considers orthosis-patient interaction forces and the ZMP criterion. In this way, it is allows the patient to modify the gait-pattern as his/her degree of voluntary locomotion still maintaining the walking stability. Three neural networks are used to decrease the time-consuming computation of the model and ZMP: the first one approximates the model-dependent term, while the second one works in the optimization procedure. Finally, the third NN reproduces the trajectory generator, decreasing the time consumed in the ZMP optimization. Also, a robust controller is proposed to attenuate the deviations from the desired trajectories due to external disturbances and parametric uncertainties. The simulations show that the proposed adaptation algorithms give satisfactory results and it can be applied in the actual exoskeleton being constructed.

8. ACKNOWLEDGEMENTS

This work is supported by FAPESP(Fundação de Amparo à Pesquisa do Estado de São Paulo) under grant 2008/09530-4 and .

9. REFERENCES

Ferris, D. P., Sawicki, G. S. and Domingo, A. R. , 2005. Powered lower limb orthoses for gait rehabilitation, *Top Signal Cord inj. Rehabilitation* **11**(2): 34–49.

Gomes, M. A. and Siqueira, A. A. G. , 2009. Neural network-based gait adaptation algorithms for lower limbs active orthoses, *Proceedings of the Summer Bioengineering Conference (SBC09)*, Squaw Valley, CA, USA.

Huang, Q., Yokoi, K., Kajita, S., Kaneko, K., Arai, H., Koyachi, N. and Tanie, K. , 2001. Planning walking patterns for a biped robot, *IEEE Transactions on Robotics and Automation* **17**(3).

Jezernik, S., Colombo, G., Keller, T., Frueh, H. and Morari, M. , 2003. Robotic orthosis Lokomat: A rehabilitation and research tool, *Neuromodulation* **6**(2): 108–115.

Jezernik, S., Colombo, G. and Morari, M. , 2004. Automatic gait-pattern adaptation algorithms for rehabilitation with a 4-dof robotic orthosis, *IEEE Transactions on Robotics and Automation* **20**(3): 574–582.

Mousavi, P. N., Nataraj, C., Bagheri, A. and Entezari, M. A. , 2008. Mathematical simulation of combined trajetory paths of a seven link biped robot, *Applied Mathematical Modelling* **32**: 1445–1462.

Riener, R., Lünenburger, L., Jezernik, S., Anderschitz, M., Colombo, G. and Dietz., V. , 2005. Patient-cooperative strategies for robot-aided treadmill training: First experimental results, *IEEE Transactions on Neural Systems and Rehabilitation Engineering* **13**(2): 380–394.

Siqueira, A. A. G. and Terra, M. H. , 2004. Nonlinear and markovian $\mathscr{H}_\infty$ controls of underactuated manipulators, *IEEE Transactions on Control Systems Technology* **12**(6): 811–826.

Siqueira, A. A. G. and Terra, M. H. , 2006. Nonlinear $\mathscr{H}_\infty$ control applied to biped robots, *Proceedings of the 2006 IEEE Conference on Control Applications (CCA06)*, Munich, Germany.

Vukobratovic, M. and Juricic, D. , 1969. Contribution to the synthesis of biped gait, *IEEE Trans. Bio-Medical Engineering* **BM-16**(1).

Walsh, C. J., Paluska, D. J., Pasch, K., Grand, W., Valiente, A. and Herr, H. , 2006. Development of a lightweight, underactuated exoskeleton for load-carrying augmentation, *Proceedings of the 2006 IEEE International Conference on Robotics and Automation*, Orlanda, Florida.

Winter, D. A. , 1990. *Biomechanics and motor control of human gait*, 2 edn, John Wiley Interscience.

Wu, F., Yang, X. H., Packard, A. and Becker, G. , 1996. Induced $\mathscr{L}_2$-norm control for LPV systems with bounded parameter variation rates, *International Journal of Robust and Nonlinear Control* **6**(9/10): 983–998.

10. RESPONSABILITY NOTICE

The author(s) is (are) the only responsible for the printed material included in this paper